

High-resolution STEM imaging with a quadrant detector—Conditions for differential phase contrast microscopy in the weak phase object approximation



S. Majert, H. Kohl*

Physikalisches Institut und Interdisziplinäres Centrum für Elektronenmikroskopie und Mikroanalyse (ICEM), Westfälische Wilhelms-Universität Münster, Wilhelm-Klemm-Straße 10, 48149 Münster, Germany

ARTICLE INFO

Article history:

Received 31 March 2014
Received in revised form
24 September 2014
Accepted 29 September 2014
Available online 8 October 2014

Keywords:

Differential phase contrast
DPC
STEM
High resolution

ABSTRACT

Differential phase contrast is a contrast mechanism that can be utilized in the scanning transmission electron microscope (STEM) to determine the distribution of magnetic or electric fields. In practice, several different detector geometries can be used to obtain differential phase contrast. As recent high resolution differential phase contrast experiments with the STEM are focused on ring quadrant detectors, we evaluate the contrast transfer characteristics of different quadrant detector geometries, namely two ring quadrant detectors with different inner detector angles and a conventional quadrant detector, by calculating the corresponding phase gradient transfer functions. For an ideal microscope and a weak phase object, this can be done analytically. The calculated phase gradient transfer functions indicate that the barely illuminated ring quadrant detector setup used for imaging magnetic fields in the specimen reduces the resolution limit to about 2.5 Å for an aberration corrected STEM. Our results show that the resolution can be drastically improved by using a conventional quadrant detector instead.

© 2014 Elsevier B.V. All rights reserved.

1. Introduction

Traditionally, Differential Phase Contrast (DPC) microscopy has been used to image the magnetic structure of a specimen at low to medium resolutions. In principle, DPC also allows the examination of magnetic or electric fields with high resolution. In recent experiments [1–3] DPC is used to directly measure electric fields with high resolution. The interpretation of these results has been highly controversial. To elucidate the contrast mechanism of this kind of measurement, we examine different quadrant detector geometries with respect to their contrast transfer characteristics. We restrict ourselves to quadrant detectors because this is the geometry used in the aforementioned experiments. An investigation of the contrast transfer characteristics of other detector geometries can be found in [4]. In addition, DPC contrast transfer calculations for different detector geometries in scanning optical microscopy can be found in [5].

A DPC signal can be obtained with the Scanning Transmission Electron Microscope (STEM) using a split detector [6]. In a classical interpretation of DPC, the direct electron beam is slightly tilted by magnetic or electric fields. If the direct electron beam is incident

on a segmented detector, this tilt can be converted to a difference signal proportional to the beam tilt angle, which is in turn proportional to the strength of the magnetic or electric field.

The wave interpretation of DPC states that in a periodic specimen illuminated by the electron probe of a STEM, convergent beam diffraction takes place. This gives rise to diffraction discs in the detector plane instead of diffraction spots observed for plane wave illumination. In the overlap regions of these discs, interference takes place. Detection of the overlap area between the direct beam and diffracted beams can therefore potentially yield images with lattice resolution. For a phase object however, the electron intensities in the overlap areas between the direct beam and a pair of opposing diffracted beams are in anti-phase as the electron probe is scanned across the specimen [6]. For a non-segmented detector covering the entire direct electron beam, this leads to a constant signal containing no modulation. In DPC microscopy, as suggested by Rose [7] and later by Dekkers and de Lang [6], the detector is divided into segments, each covering one of the aphasical areas. By subtracting the signals of opposing segments, an image of the gradient of the electrons phase change in the specimen is generated.

As previously mentioned, DPC is routinely used to image magnetic fields within a specimen (e.g. [8]). One possible detector geometry to image inner magnetic fields at low resolutions is shown in Fig. 1. A ring detector is divided into four quadrants and the direct electron beam is placed within the ring, only overlapping

* Corresponding author.

E-mail address: kohl@uni-muenster.de (H. Kohl).

URL: <http://www.uni-muenster.de/Physik.PI/Kohl/> (H. Kohl).

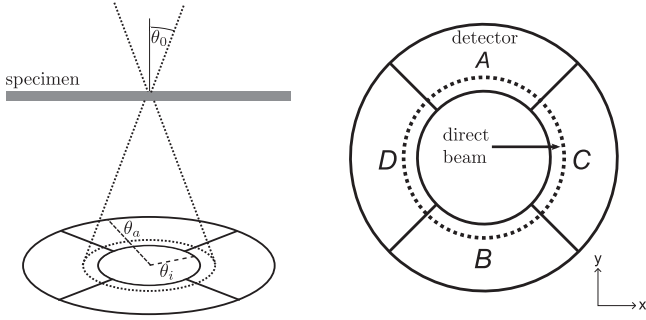


Fig. 1. Proposed detector setup for the measurement of local electric fields with high resolution DPC. The direct beam is centered on a ring quadrant detector (outer detector angle θ_a , inner detector angle θ_i) with a small overlap between the two. Two signals $S_1 = B - A$ and $S_2 = D - C$ are obtained.

a small part of the detector. Judging by the classical interpretation of DPC, this detector setup should also be suited for the high resolution imaging of electric fields, since the classical interpretation does not impose a resolution limit. To determine whether this conclusion is valid, the wave nature of the electrons has to be taken into account. For a direct measurement of electric fields with DPC, two conditions have to be fulfilled. First, the imaged object has to be sufficiently thin so that the weak phase object approximation holds. This means that its thickness has to be much smaller than the extinction distances of the crystal. This condition depends on the particular specimen and can be easily verified by a dynamic diffraction calculation. Assuming that this first condition is fulfilled, the imaging system also has to image the gradient of the object potential. To discern whether the second condition is met, the Phase Contrast Transfer Function (PCTF) is calculated in the following section and then slightly modified to yield the Phase Gradient Transfer Function (PGTF), which characterizes the contrast transfer of the object potentials gradient. Using the PGTF, a DPC resolution limit is defined, which is an estimate of the smallest structure size for which the second condition is met.

2. Theory

For a weak phase object, the PCTF $\mathcal{L}(\vec{\omega})$ is defined as [9]

$$C(\vec{\omega}) = \mathcal{L}(\vec{\omega}) \frac{2}{\lambda} F(\vec{\omega}), \quad (1)$$

where $C(\vec{\omega})$ denotes the two-dimensional Fourier transform of the contrast function, $\vec{\omega}$ is the two-dimensional scattering angle, λ the deBroglie wavelength of the electrons incident on the specimen and $F(\vec{\omega})$ the elastic scattering amplitude of the object potential. The PCTF $\mathcal{L}(\vec{\omega})$ of a STEM can be written as [9]

$$\mathcal{L}(\vec{\omega}) = \frac{i}{2\pi\theta_0^2} \int A(\Theta) D_a(\vec{\Theta}) \{A(|\vec{\omega} - \vec{\Theta}|) e^{-i\gamma(|\vec{\omega} - \vec{\Theta}| - \gamma(\Theta))} - A(|\vec{\omega} + \vec{\Theta}|) e^{i\gamma(|\vec{\omega} + \vec{\Theta}| - \gamma(\Theta))}\} d^2\Theta. \quad (2)$$

Here, $\vec{\Theta}$ is the angle towards the detector plane, while $A(\Theta)$ is the aperture function, which, in the case of a circular aperture, takes the form of

$$A(\Theta) = \begin{cases} 1 & \text{for } \Theta < \theta_0 \\ 0 & \text{for } \Theta > \theta_0, \end{cases} \quad (3)$$

where θ_0 is the objective aperture angle. $D_a(\vec{\Theta})$ is the antisymmetric detector function

$$D_a(\vec{\Theta}) = \begin{cases} \pm 1 & \text{for } \vec{\Theta} \in \pm \text{detector segment} \\ 0 & \text{otherwise.} \end{cases} \quad (4)$$

For an ideal microscope, the aberration function γ becomes zero, reducing Eq. (2) to

$$\mathcal{L}(\vec{\omega}) = \frac{i}{2\pi\theta_0^2} \int A(\Theta) D_a(\vec{\Theta}) \{A(|\vec{\omega} - \vec{\Theta}|) - A(|\vec{\omega} + \vec{\Theta}|)\} d^2\Theta. \quad (5)$$

Eq. (5) omits the influence of the source size and the lens aberrations on the contrast transfer. The source size can be taken into account by multiplying the right hand side of the equation with the Fourier transform of the source function, whereas the consideration of lens aberrations would require the numerical solution of the integral in Eq. (2) [4]. Obviously the influence of source size and lens aberrations is smaller than the point resolution achievable with a high resolution STEM (< 0.1 nm [10]). Both effects will lead to an additional damping of the transfer function, particularly at high spatial frequencies.

By exploiting the antisymmetry of the detector function $D_a(\vec{\Theta}) = -D_a(-\vec{\Theta})$, Eq. (5) can be simplified further yielding

$$\mathcal{L}(\vec{\omega}) = -\frac{i}{\pi\theta_0^2} \int A(\Theta) D_a(\vec{\Theta}) A(|\vec{\omega} + \vec{\Theta}|) d^2\Theta. \quad (6)$$

As shown in Fig. 2 for a ring quadrant detector, the integral in Eq. (6) can be interpreted as the overlapping area between a circle of radius θ_0 centered on the origin, the detector geometry $D_a(\vec{\Theta})$ and a circle of radius θ_0 with its center shifted by the scattering angle $\vec{\omega}$. Examining Fig. 2 shows that, if θ_0 is larger than the outer detector angle, the calculation of the cutting area between the detector geometry and the shifted circle is sufficient to evaluate the integral in Eq. (6). If the objective aperture angle θ_0 is smaller than the outer detector angle, the integral can still be reduced to the cutting area between the detector geometry and the shifted circle, provided that the outer detector angle is replaced by the objective aperture angle in the resulting equation.

Dividing the detector geometry into semicircles as shown in Fig. 3 allows a further simplification for the calculation of the intersection area to the overlapping area between a semicircle and a circle (with arbitrary radii). This area can be calculated using elementary geometry, leading to the equations given in the appendix.

By combining the results in the appendix according to Fig. 3 and dividing the result by $\pi\theta_0^2$, the PCTF as described in Eq. (6) can be obtained. To get a better impression of the DPC transfer, the PGTF

$$\tilde{\mathcal{L}}(\vec{\omega}) = \frac{\mathcal{L}(\vec{\omega})}{i\omega_x} \quad (7)$$

is plotted in the following section rather than the PCTF. The division by $i\omega_x$ in Fourier space corresponds to an integration in real space, which means that the PGTF can be directly compared to the contrast transfer functions of non-differentiated contrast mechanisms. However, in contrast to the PCTF, the PGTF does not describe the transfer characteristics of the electrons phase change in the specimen

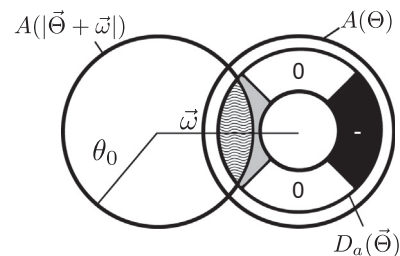


Fig. 2. Visualization of the integral in Eq. (6) for two opposing segments of a ring quadrant detector. The solution of the integral is the area of overlap between the two circles and the detector function, which is highlighted by wavy lines in the picture. For smaller values of ω than shown in the picture, any potential overlap with the negative part (right quadrant) of the detector function has to be subtracted from the overlap area with the positive part (left quadrant) of $D_a(\vec{\Theta})$.

Download English Version:

<https://daneshyari.com/en/article/8038223>

Download Persian Version:

<https://daneshyari.com/article/8038223>

[Daneshyari.com](https://daneshyari.com)